Wind Tunnel Results for the Mobile Temperature Sensor (MTS)
(Proprietary data of Global Aerospace, LLC and SpectraSensors, Inc.)

Rex J. Fleming and Randy D. May

April, 2006

1. Introduction

The Kirsten Wind Tunnel, part of the University of Washington Aerodynamic Laboratory (UWAL), located on the U. of W. campus in Seattle, Washington, was open for testing in 1939. The aging facility has an atmosphere typical of most universities. Old block walls and metal steps are the décor – giving the feeling of heavy use in the past, and concern whether it is still being used. In fact, it is still being used by a range of users, from individuals concerned with umbrella design to the Boeing Company who use it often.

The facility is on the U. of Washington campus about 20 miles from the Seattle-Tacoma (Sea-Tac) International Airport. The tunnel operator's console has controls for operating the tunnel, changing speed, changing model attitude, and acquiring data. The tunnel is a double-return closed circuit design. Two 500-hp dc motors drive two seven blade fans to provide the test section with wind speeds of up to Mach = 0.25. Each blade is made of Honduras mahogany. Each fan has a diameter of 14 feet 9 inches with approximately a ¼ inch clearance between the blade tip and tunnel wall. The accuracy of the Mach number is +/- 0.01 %. The test section of the tunnel has a rectangular cross-section 8' high, 12' wide, and 10'long with 1.5'high fillets (45 degrees) in all for corners. The test section is on the second floor of the building – level with the observation deck and the model deck.

Our use of the wind tunnel was to test several aspects of the Mobile Temperature Sensor (MTS). **The goal of the MTS is to measure the outside or ambient air temperature from mobile platforms [a range of airborne platforms from UAVs, small general aviation aircraft, business aircraft, commercial turboprop aircraft, commercial jet aircraft, and a variety of military aircraft]. The sensor must be (1) extremely accurate, (2) operate for a long period of time without repair or re-calibration, (3) be located as a flush mounted sensor on the side of the fuselage (thus, no heater required by the FAA and providing: greater accuracy for users; less heater maintenance expense for air carriers; less drag, thus, more fuel savings for air carriers; and a more stealthy profile for military aircraft). This MTS sensor eliminates all the above problems with the current BF Goodrich aircraft total air temperature (TAT) probe.**

The testing is subject to the laws of physics for compressible flow of a caloric perfect gas. These equations are well understood. The thermodynamic processes are isentropic (adiabatic and reversible) except in thin viscous boundary layers with friction.

In view of the apparent contradiction of trying to measure the ambient temperature within a friction layer surrounding the skin of a fast moving aircraft, a road map indicating the obstacles to be faced and how they will be overcome is in order. The measurement made with the MTS is more than a centimeter away from the aircraft skin. The friction effect is significant but not overwhelming. The effect of friction will be isolated through the design and physical insulation of the measurement cell area. Thus isolated, the effect of friction will be modeled as a function of Mach number.

The modeling can very effectively be accomplished with today's computers, algorithms, and special statistical processes (described later). Many simulations, accounting for all manner of expected problems, have been performed which suggest that this process will indeed work and will provide accurate static or ambient atmospheric temperature.

The modeling of the **temperature increase or ΔT due to friction** will be performed as a function of a polynomial in Mach number (M). This can be in two forms:

$(\Delta T)_{\mathbf{TS}} = A1 + A2\,M + A3\,M^2$ a quadratic form (or a higher order polynomial) where the subscript **TS** indicates that a **static temperature sensor** is used or by the form:

$(\Delta T)_{\mathbf{TT}} = A1 + A2\,M + A3\,M^2$ a quadratic form (or a higher order polynomial) where the subscript **TT** indicates that a **total temperature sensor** is used.

The concept of the total temperature has proven useful for some but not all aspects of aerodynamic applications in a **compressible fluid** (which must be assumed when the Mach number is greater than M = 0.3 -- with M = 1 being the speed of sound).

The total temperature concept is that a fluid element moving at velocity (V) has a total temperature **associated** with the fluid element but an **actual** pressure and temperature equal to P and T, respectively. The actual P and T are called static pressure (PS) and static temperature (TS), respectively, and it is not until the fluid element is brought to V = 0 (by a sensor that stops the flow) **in an isentropic process** that the total temperature (TT) is **realized.** With this definition the total temperature (TT) is related to the static temperature (TS) by the following equation

$$TT = TS\,(1 + 0.2\,M^2).$$

The above equation is based upon a reversible thermodynamic process (one in which no dissipative processes occur, i.e., where the effects of viscosity, thermal conductivity, and mass diffusion are absent). Here is another contradiction. Can one use a TT sensor in a situation with friction when the TT concept is not defined when friction is present?

The purpose of these initial wind tunnel tests is first to observe just what does occur within the friction domain. It may not matter what the actual relationships are as one can always model the ΔT due to friction with real data supplying the actual TS and additional data from the TS sensor, the TT sensor, or both. Thus, first we observe then we apply what we have learned

The organization of this test summary includes a brief review of the MTS and discusses the data processing in Section 2. Section 3 will reveal what was measured and other related aspects of the properties of the MTS. Section 3.1 describes the rapid up and down cycles of Run04 which take the Mach numbers from a small warm up value to a peak value and then down again. **Three different Mach peaks are achieved in this cycle.**

Section 3.2 covers the results from a much longer stair step run with a cascade of flow values to a higher plateau of values, holding these for a period of time, then going higher to the next level – eventually peaking at a maximum value -- and returning back down again. Section 3.3 provides the results of a hybrid UCAR air sampler with the lower level flow blocked off. Tests with this hybrid system and the MTS reveal just how well the total temperature (TT) can be measured. Section 3.4 describes the aerodynamic and thermodynamic characteristics of the air sampler. Section 3.5 discusses the ambient temperature (TS) results.

Section 4 will indicate the modeling results for TS using the data measured and compare the accuracy of the modeled friction correction versus the measured data. Section 5 provides a brief summary and conclusion.

2. Review of MTS and Data Processing

The original basis of the MTS is Dr. Fleming's invention of the flush mounted air sampler (United States Patent No. 6,809,648 B1) – see Fig. 1 below. This air sampler (which has virtually no drag and requires no heater) has been successfully combined with a diode laser system developed Dr. Randy May, co-founder of SpectraSensors, Inc (SSI), to measure atmospheric water vapor.

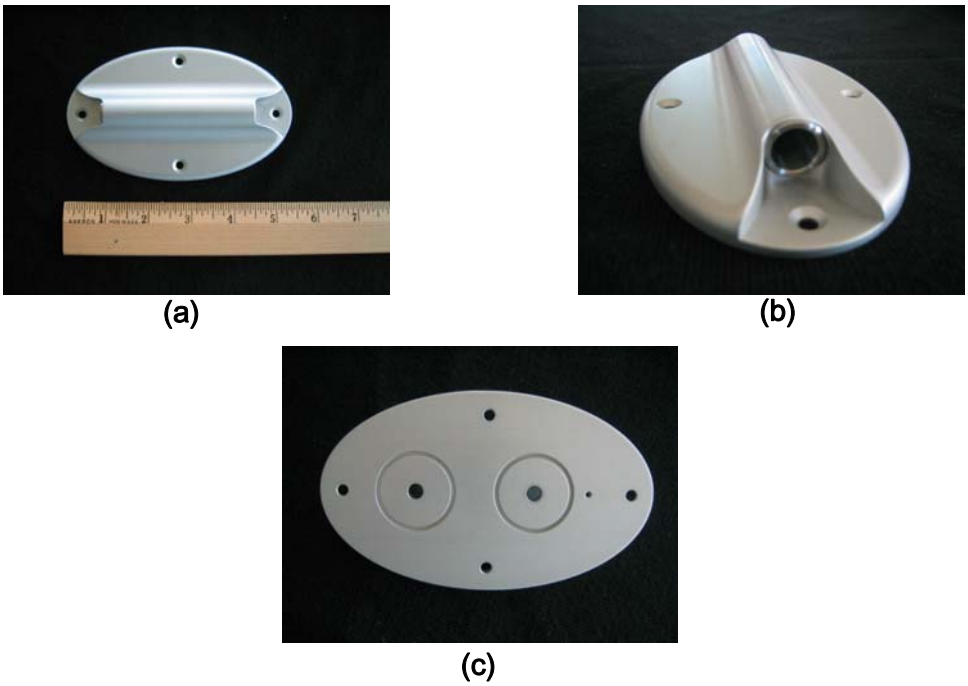

Figure 1. Three views of the air sampler: (a) top, (b) oblique, and (c) bottom.

This system, called the Water Vapor Sensing System (WVSS-II) is being used operationally by the United Parcel Service (UPS) on B-757 cargo aircraft. The second invention of Dr. Fleming (patent pending) is the MTS where the air sampler shown in Fig.1 is modified to perform the temperature measurement while maintaining the original flow characteristics of the air sampler.

Fig. 2 indicates the construction of the MTS. This reveals the modification of the original air sampler where the hoses to an internal measurement cell for lasers are replaced by a solid metal measurement cell containing two temperature sensors. Fig. 2 shows that the extruded measurement cell is mounted to the required doubler/filler plate necessary for the aircraft (or mobile platform) to maintain its original structural integrity.

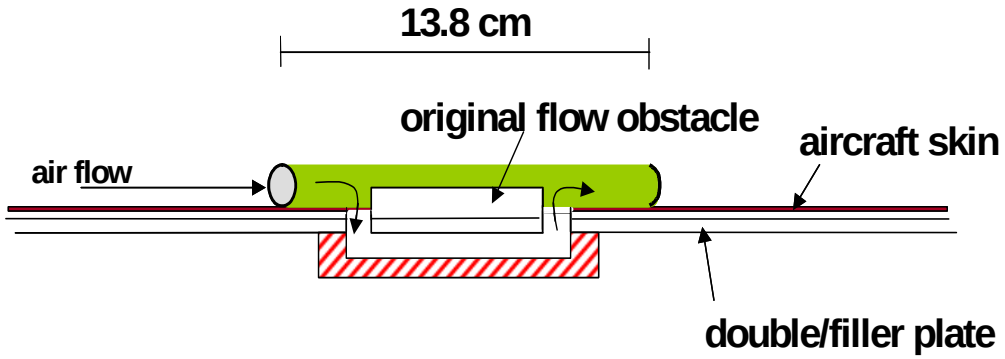

Figure 2. Cut-away side view of metal (aluminum or composite) extrusion.

Air carriers use both ambient (or static) temperature (TS) and dynamic or total temperature (TT). The aircraft measures the Mach number (M) with the pitot tube providing static and dynamic pressure. With accurate TT, the TS is computed by the formula (where the temperatures are always in degrees Kelvin):

$$TT = TS\,(1 + 0.2\,M^{2}) \qquad (1)$$

The MTS provides both temperature measurements. **However, the MTS could have two very accurate static temperature measurements and use the Mach number to compute the dynamic temperature.** Many scientists throughout the world have been concerned that the **current reverse process** (TT measured by Goodrich and then converted to TS) is producing TS values with large biases and random errors. This is the reason for the demand for this MTS product.

Fig. 3 shows another perspective of the measurement cell, which has a hollowed out volume (extrusion) like a “tub”. The current TS sensor is located within the wall of the tub and the TT sensor is located in the interior flow area. This measurement area could contain two static temperature sensors measuring TS (both located on each side of the tub area recessed (imbedded) with the walls 5/1000 of an inch). **This will be the final version of the MTS.**

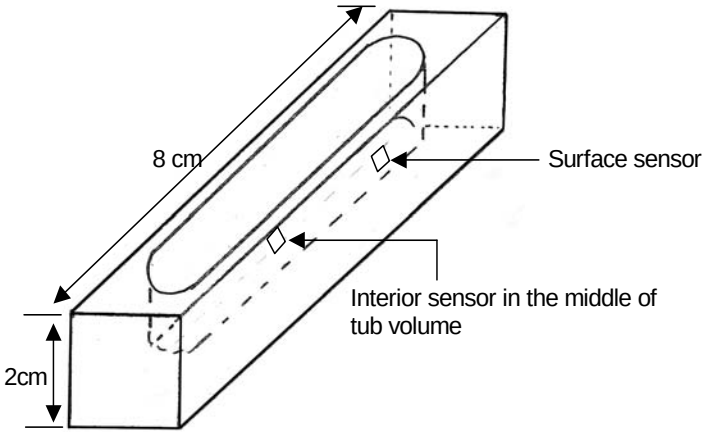

Figure 3. The bottom portion of the MTS (measurement area).

The current configuration, with the TS and TT sensors indicated as in Fig. 3 was the version that was tested and described here. **This version produces the maximum information needed to make a final decision on the final design.**

A limitation of this wind tunnel is the one static temperature sensor located in the active test area. The beginning of each test (especially during the early morning tests of the MTS) leads to an immediate drop of the static temperature as cooler air from the back of the wind tunnel is brought forward to the test area. The two PRT temperature sensors within the MTS are extremely sensitive and both clearly indicate this cooling as the wind tunnel motors are first turned on. Thus, the initial records must be removed until the temperatures become more homogeneous and begin to increase. The end of the record is also removed when Mach numbers are quite low due to random error in the UW sensor (accurate to only one degree (F)). Any warming trend in the tunnel test area is removed from the remaining data – always being sure that the temperatures are dynamically consistent. This means that TT is greater than the TS values at all Mach numbers.

Another software tool used is singular value decomposition (SVD) to model the various temperatures as a function of Mach number. Since the data records used are after the warm-up period, there is no actual data with M = 0. However, by modeling the various temperature values as quadratic functions of Mach number (M) one obtains the estimated value of temperature when M = 0. This is discussed further in Section 3.1.

The data provided by UWAL for this run were about 4 seconds apart. The data gathered by the MTS system is much faster (a variable rate of between 1.8 and 2.2 Hertz or about 2 data points per second or about 8 times as much data as the UWAL provided). Using the UWAL data set, the **Mach number** and **static temperature (tsuw)** were bilinear interpolated to provide all the variables of interest at the high data collection rate of the MTS system (now all data have the same time and Mach #s). This will imply that the (tsuw) data shown below is as accurate as the MTS sensors, but this is clearly not the case. This interpolation was performed for all the runs described in this summary.

3. Observations and Relationships

Figures 4 and 5 are pictures within the test area (Randy May is behind glass door of viewing area along with a technician communicating with wind the tunnel control staff). The MTS is mounted on a plate which is mounted on a bicycle mount (surfboard shape).

Figure 4. Wind tunnel test area.

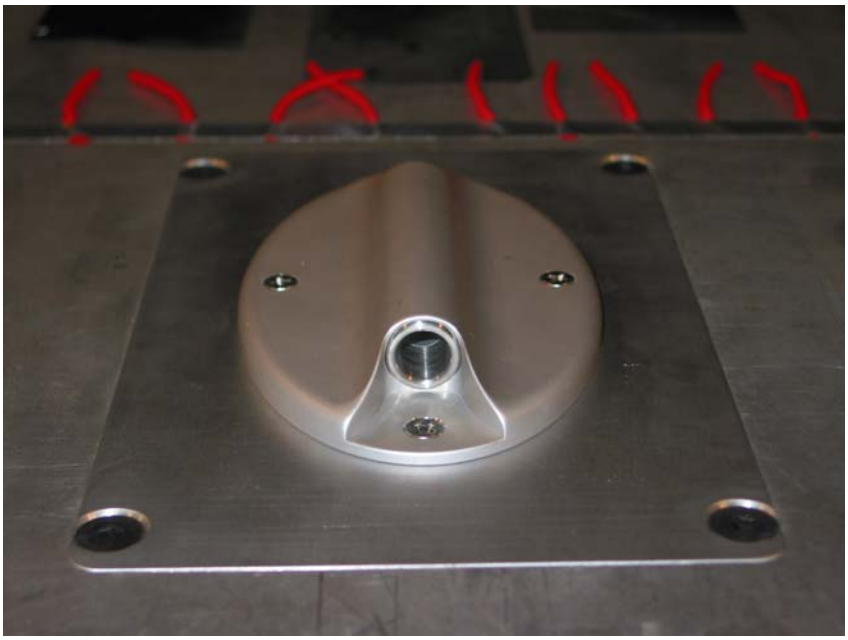

Figure 5. Close up of MTS on plate on bicycle mount.

Sub-sections (3.1 through 3.5) contain the important observations and relationships.

3.1 Rapid Up and Down Cycle with the MTS (Run04)

TheRun04 data is the MTS system run through several peaks of rapid Mach number increase and decrease. Three different Mach number peaks are achieved and then the wind strength is reduced. The processing of the data as described in Section 2 results in the data shown in Fig. 6 below. **[All figures have temperatures in centigrade – these are put into degrees Kelvin (T (K) = T(C) + 273.15) when required.]**

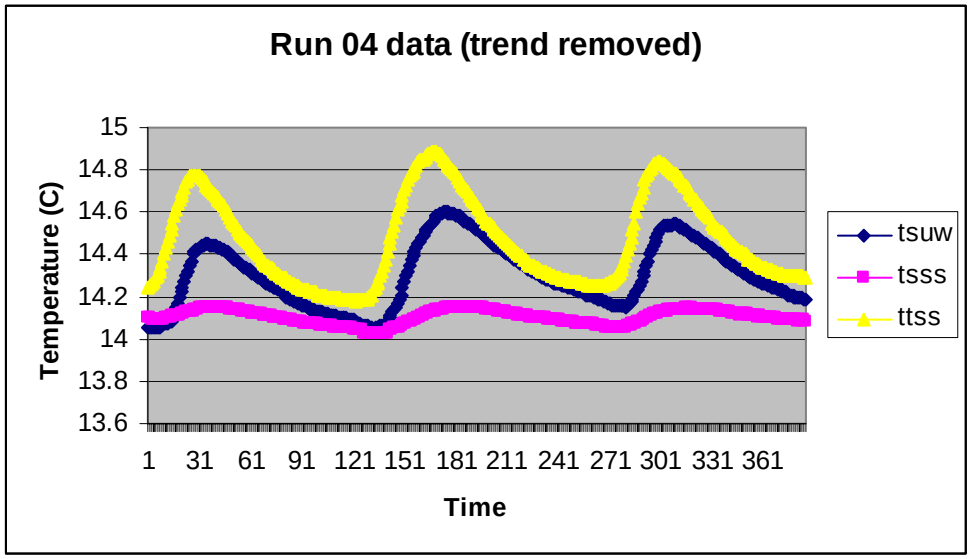

Figure 6. Run04 data as indicated.

Fig. 6 indicates several important points: the effect of the heating in the wind tunnel and several aspects of the system design that we want to achieve. The first obvious effect seen is the residual warming within the wind tunnel (even with the warm trend removed) after each of the three Mach peaks is reached. This result would not be seen in the operation of the sensor on a jet aircraft in the open atmosphere. The response time of the two temperature sensors within the MTS is extremely fast – what is seen is the heat trapped within the finite enclosed test area of the wind tunnel.

Fig. 6 shows the amplitude of the three temperature records as expected. The highest peak (**yellow**) is the "total temperature" (TT) from the MTS which is referred to as the total temperature from SpectraSensors (ttss). This is the total temperature measured within the MTS "tub area" This is will be a function of the air speed (Mach number) **similar** to Eq. 1. The second highest peak (**blue**) is the static temperature of the wind tunnel test area (tsuw). This is primarily due to the friction of the wind speed in the test area the (effects of walls, floor, ceiling, and model deck.), and other minor thermal sources.

The final curve (**pink**) in Fig. 6 is the static temperature (TS) within the MTS. These data have the lowest amplitude for several reasons. The primary reason is that the ambient wind tunnel air, initially heated (see above), is also reduced by the cooling induced by the taper design in the entrance to the air sampler (discussed further below). Thus, the blue curve (wind tunnel heating) does affect the pink curve as warmer air is passing through the MTS. Again, in the real world of a mobile platform within the atmosphere, the MTS will be measuring the ambient atmospheric temperature (without the wind tunnel frictional heating).

The MTS will measure TS plus an additional heating due to skin friction of the fast moving aircraft (or mobile platform). **The effect of the friction is isolated and modeled as a function of Mach number to reproduce the actual atmospheric temperature.** The isolation of the friction occurs because of the avoidance of additional heating (from both inside and outside the aircraft) by the insulating features surrounding the measurement cell.

The modeling of the friction is done by fitting a polynomial in Mach number (M). For example, the measured static temperature in the cell can be modeled as:

$$TSSS = A1 + A2 * M + A3 * M^2$$

This is a second order polynomial in M. One can go to higher order polynomials and many simulations using singular value decomposition (SVD) and sophisticated residual error analysis have been performed that suggest that the atmospheric value can be obtained to within +/- 0.3 C – given the temperature sensors within the MTS which are accurate to +/- 0.1 C. The sensors used are platinum resistance thermistors (PRTs). They Are 1000 Ohm, 2mm square , 1mm thick (thin film encased in ceramic) sensors – imbedded in the tub walls for further protection from the intrusive environment.

An example of using SVD to model each of the temperatures during Run04 is provided below. Recall that the initial cooling during the wind tunnel runs precluded the use of the data at low Mach numbers. However, the power of the SVD method is such that the answer provided by the solution for A1 in the polynomial equation above provides the expected temperature at M = 0, a value which is consistent with the data provided.

The results for this Run04 for the various temperatures are shown below:

$$TSUW = 14.01 + 1.48\ M + 0.58\ M^2$$

$$TSSS = 13.92 + 1.09\ M - 2.45\ M^2$$

$$TTSS = 14.29 - 1.32\ M + 15.36\ M^2$$

One can further apply residual error analysis to these results to remove **data outliers.** For example, if the **data** used (TSUW or TSSS or TTSS) is referred to as YDATA and the SVD **modeled value** for the same variable is called YMOD, then one can calculate

YDIF (i) = Absolute value of [YMOD(i) – YDATA(i)] for each data point (i)

YDIF% (i)= [YDIF(i) / YDATA(i)] *100. = error as percent of signal for each point (i).

One can then eliminate data points greater than a threshold value say (e.g., 90%) of the maximum value of YDIF% (i) for all (i). **The points that remain are then used again in a new SVD run to obtain a better model without the outliers.**

A systematic removal of points greater than ZTEST * MAX (YDIF%) is performed where ZTEST is lowered from 99% to some lower value (84% in the case shown below). This **simple** residual analysis was performed on the RUN04 temperature values and a slightly different set of values result for the polynomial coefficients as shown below:

$$TSUW = 13.96 + 2.27\ M - 1.50M^2$$

$$TSSS = 13.90 + 1.36\ M - 3.29\ M^2$$

$$TTSS = 14.26 - 0.78\ M + 13.81\ M^2$$

Note that the static temperature values (TSUW and TSSS) have virtually the same value at M = 0. The total temperature value (TTSS) is initially about 0.3 degrees warmer. This is not a large difference but perhaps significant as discussed in Section 3.3. Using these new polynomial values, the resulting temperatures are plotted as a function of Mach number as seen in Fig. 7 below.

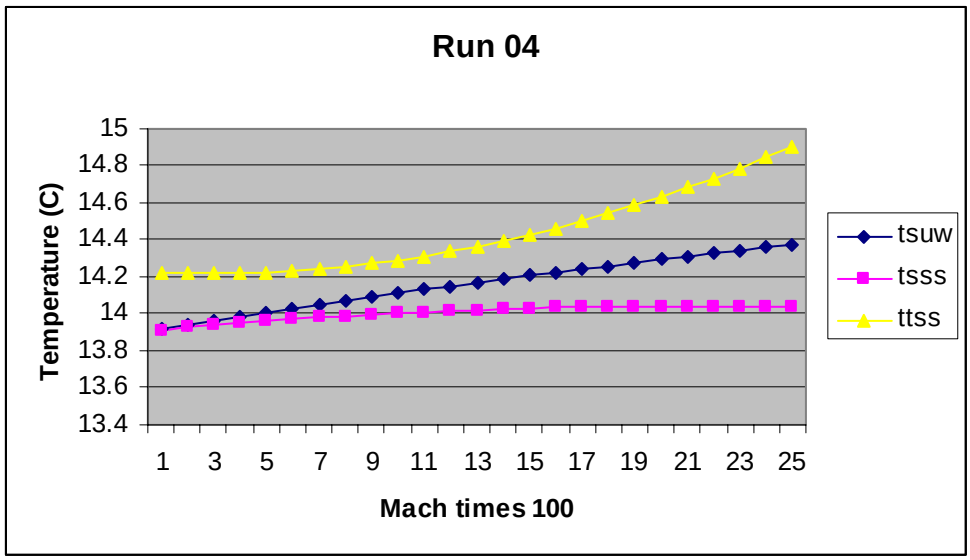

Figure 7. Run04 results for the various temperatures (after residual outlier analysis)

The three curves have their proper relative amplitudes, while the initial value for the ttss curve is **slightly** higher. This is discussed further in Section 3.3.

3.2 Further Wind Tunnel results (slow stair step up and down)

After two trial runs with the wind tunnel staff checking their equipment, the first real test in the wind tunnel was Run 03. This was a long test of stepping the wind speed up to a certain level, holding it there for 25 seconds or so, then stair stepping up in a similar manner to the maximum possible speed, then back done again in the same fashion. The actual data collected by UWAL was about 30 minutes worth, but we ignored the early and late portions which were at low Mach numbers and contaminated with initial cooling and late warming. Our data used for this test run was approximately 20 minutes in length compared to the 4 minutes for the Run 04 described in Section 3.1.

This early morning test had more initial cooling than the later Run 04. Moreover, since the length of the run was so much longer by comparison, the warming within the wind tunnel over time was significantly greater. This meant that the trend removal was far greater as seen in the figure below where temperatures are lowered within each plateau.

Fig. 8 shows the left half of the ramp up of the actual data used. Here the transient data between the steps has been removed. **The run is referred to as Run33 (as opposed to the original Run 03 with the transient data included – the results are not substantially different but the record is just longer and less interesting to plot).** Again we see the proper order of the data with the largest magnitude for the dynamic total temperature (**yellow**), followed by the UWAL static temperature (**blue**), and finally the MTS static temperature (**pink**). The warming in the wind tunnel test area (**blue**) is strong (close to the total temperature measured) and influences the static measurements of the MTS.

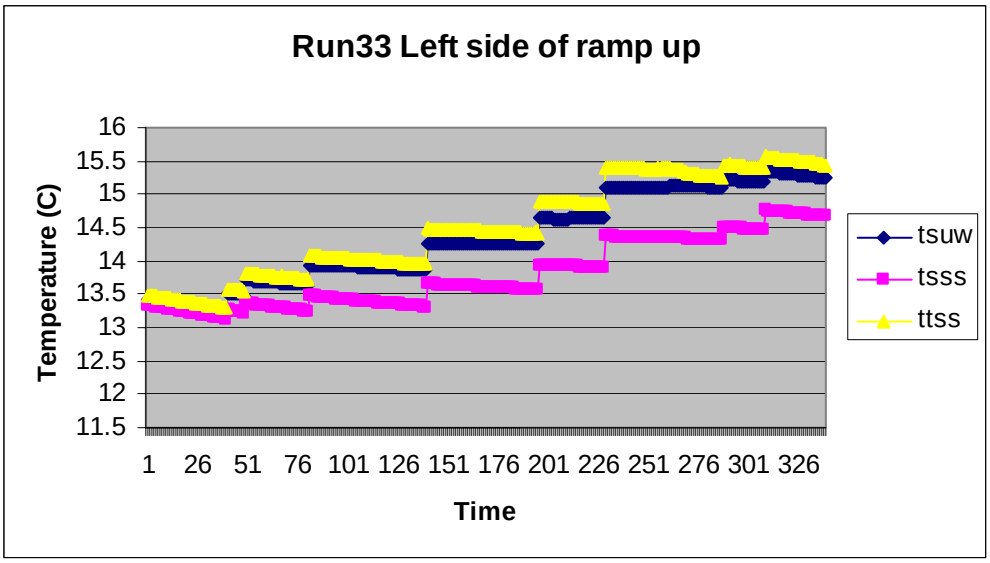

Figure 8. Left side of ramp up of Run 03 (called Rn33 with transient data removed)

Although not discernable in Fig. 8, the wind tunnel controls slowly allow the Mach number to drift downward slightly at each of the desired "stationary" levels before increasing in value to the next level. This produces a very poor data set from a mathematical and physical perspective. Mach number is going down and temperature is going up which produces inconsistent data. Trend removal makes this inconsistency smaller, but the polynomials generated are substantially different for Run 3 than those produced for Run 4. This is discussed further in Section 4.

The SVD model values for the temperatures for this run are provided in Fig 9. The same relative order of magnitude is seen in the temperature curves as in Fig. 7 for the Run 04.

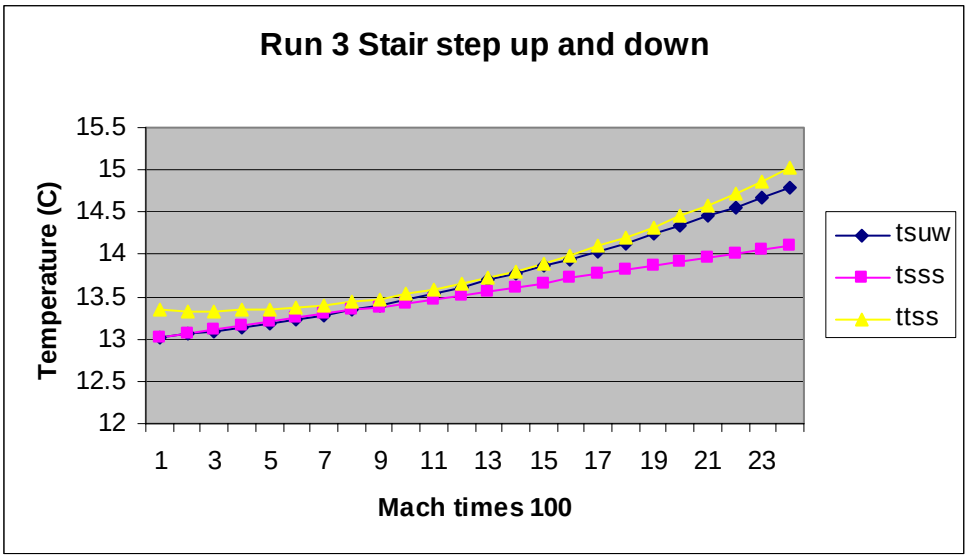

Figure 9. The temperature curves from SVD modeled data

3.3 Determining the Total Temperature (TT) from MTS and Hybrid System

Another air sampler (exactly the same except that the flow to the lower tub area was blocked off) was used with a temperature sensor in the upper area to measure TT. This hybrid system was used in Run 07 (similar to Run 04 with a rapid ramp up and down with three Mach number peaks). Results of Run 07 are shown in Fig. 10 for the temperature measured (TTSS) and the provided UWAL static temperature (TSUW).

Recall from the Introduction that the TT we are purporting to measure is not truly the TT by definition because of the contradictory friction involved. Nevertheless, one can compare what is measured by the TT sensors and see what relationships exist, if any.

Both Fig. 7 and Fig. 9 which were based upon the SVD modeling and residual analysis revealed that the TTSS values at M = 0 were offset from the nearly identical values for TSUW and TSSS at M = 0. Fig. 10 also indicates that the TTSS value is higher than the TSUW value at M = 0. This initial difference is 0.2 degrees C as seen in the polynomial values below.

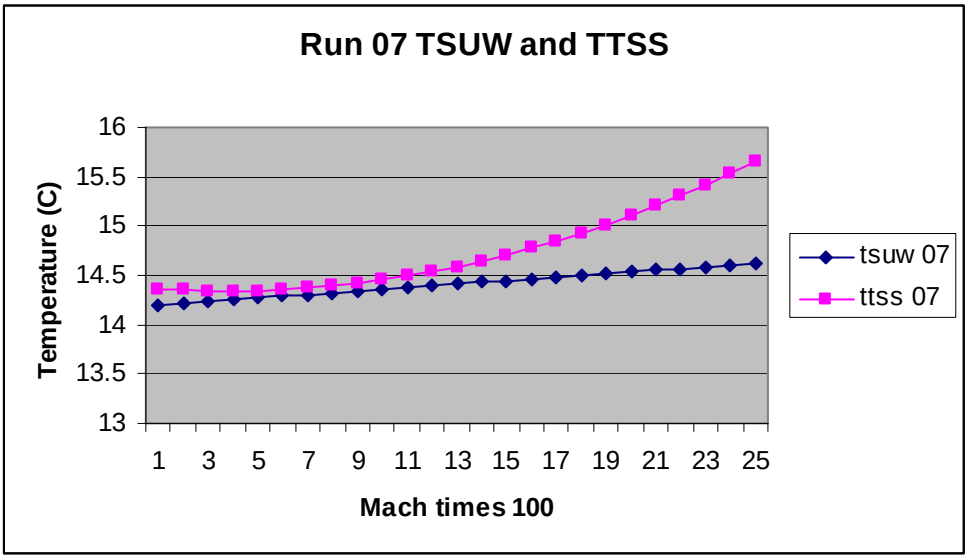

Figure 10. Run 07 with air sampler flow blocked in lower level.

The results from the SVD calculations for Run 07 are shown below – along with the previous results for Run 04 and Run 03 to complete Table 1.

$$TSUW = 14.18 + 1.832\ M - 0.2791\ M^2 \qquad \text{[Run 07]}$$

$$TTSS = 14.38 - 2.140\ M + 28.90\ M^2 \qquad \text{[Run 07]}$$

$$TTSS = 14.26 - 0.787\ M + 13.81\ M^2 \qquad \text{[Run 04]}$$

$$TTSS = 13.32 - 6.039\ M + 63.02\ M^2 \qquad \text{[Run 03]}$$

From the discussion in the Introduction, the TT measured from the TT sensors in both the MTS and the hybrid system are not the TT for isentropic flow. Clearly one would not use the friction-heated value of TSUW at each data point as the TS in Eq. 1 (assuming that this equation even applies). **But one can use the initial TS value from the SVD results for M = 0 in Eq. 1. This is what is compared in Table 1.**

The first column in Table 1 indicates the various events, runs and appropriate Mach Peaks (P). The second column gives the Mach # for that (P). The third column is the **measured (TT).** The fourth column is the (TT) based upon the A1 coefficient [M = 0 or the (TS) from the SVD for (ttss)]. The fifth column is the (TT) based upon the A1 coefficient [M = 0 or the (TS) from the SVD for (tsuw)]. The last two columns give the percent of the measured value compared to the previous two TT columns.

The results are somewhat surprising in that the measured TT is not far off the value that one would expect if the isentropic total temperature relationship (Equation 1) were valid.

Using the values above, the **measured values of TT** range from 99.06 to 99.56 of the values for TT from Eq. 1 with the TS values coming from the SVD A1 values for **TTSS** for the various runs and Mach peaks. Similarly, the measured values of TT range from 99.17 to 99.61 of the values for TT from Eq. 1 with the TS values coming from the SVD A1 values for **TSUW** for the various runs and Mach peaks.

Event	Mach #	Temp (TT) Measured (M)	Temp (TT) SVD (ttss)	Temp (TT) SVD (tsuw)	% (M / ttss)	% (M / tsuw)
04 P1	**0.23573**	**287.92**	**290.60**	**290 .39**	**99.08**	**99.18**
04 P2	**0.24153**	**288.04**	**290.76**	**290.55**	**99.06**	**99.17**
04 P3	**0.23498**	**287.99**	**290.58**	**290.37**	**99.11**	**99.21**
03 P1	**0.24881**	**288.75**	**290.02**	**289.88**	**99.56**	**99.61**
07 P1	**0.23104**	**288.68**	**290.60**	**290.40**	**99.34**	**99.41**
07 P2	**0.23355**	**288.57**	**290.67**	**290.46**	**99.28**	**99.35**
07 P3	**0.23223**	**288.52**	**290.63**	**290.43**	**99.27**	**99.34**

Table 1. Total Temperatures (TT) for the various runs as indicated (see text).

An often misunderstood aspect of this type of flow, is that even with the much slower speed in the lower level measurement area of the MTS (perhaps only 16 -18% of the flow in the upper level of the hybrid system according to simulations), both TT sensors still measures the same proportionate TT despite the flow speed differences.

This is also seen in the Goodrich TAT probe where the flow in the measurement area is slowed to about M = 0.3 to 0.35 to optimize the recovery factor of the TT measurement. Despite the slowed flow in the measurement area, the sensor measures the correct TT at its full Mach value. One sees from Table 1 that both the TT from the MTS and from the hybrid system measure similar TT values.

There is another method for checking the "effective flow" between the hybrid and the MTS. The means of calculating this flow uses the notation TT7, TS7, and M7 = TT, TS, and Mach number from Run 07, respectively, and TT4, TS4, and M4 = TT,TS, and Mach number from Run 04, respectively, is as follows. **Assuming that Eq. 1 holds,** one has

$TT7 = TS7\ (1+0.2\ M7^{2})$ and $TT4 = TS4\ (1+ 0.2M4^{2})$ and if $TS4 = C\ (TS7)$
where C = the ratio of TS4/TS7 in degrees Kelvin, then it can be shown that:

$$M4 = SQRT \left[\{ [TT4 (1+0.2M7^2) / C (TT7)] - 1 \} / 0.2 \right]$$

The value of C will usually be close to 1 and the actual value for C = 0.99958 from the SVD values for Run 07 and 04 above. Substituting Run 03 for Run 04, the value of C = 0.995, but the value of TT3 provides the somewhat surprising result below.

Using the values from the SVD calculations above, the **effective** flow in the lower portion of the air sampler (from Run 04 or Run 03) is indicated in Table 2. Note that the values are entirely dependent upon the SVD values calculated and the assumption that Eq. 1 actually holds.

Mach #	**% of effective flow in MTS**	
	Run 04	**Run 03**
0.15	**94.6**	**108.8**
0.20	**92.4**	**107.8**
0.25	**91.1**	**107.7**
0.30	**90.2**	**107.9**

Table 2. Calculated effective flow in air sampler as function of Mach # .

3.4. Aerodynamic and Thermodynamic Properties of the Air Sampler Taper

The aerodynamic taper and flow obstacle in the entry portion of the air sampler are not shown in Fig.1, but the obstacle is indicated in Fig.2. Together these act as an inertial separator. The taper shape and obstacle height were designed to produce maximum conditions for the WVSS-II water vapor measurement. Many simulations were performed by varying these parameters to achieve the desired results.

The inertial separator helps remove particles more dense than water vapor that might interfere with the **sensitivity** (not accuracy) of the laser sensor for water vapor in upper layers of the atmosphere. Undesirable particles include new snow (a factor of 10 more dense than water vapor), snow crystals (a factor of 100 more dense), aerosols (up to 1000 times more dense), and various biological entities (insects, bird entrails [problem for the Goodrich TAT probe -- less likely a problem for the low profile, flush mounted MTS], etc). The simulations of the air sampler suggest a range of 82-95% of the particle volume being removed. The removal of the above particles would also extend the lifetime of an MTS with a TT sensor inside (though the final design is two TS sensors).

The aerodynamic taper will accelerate an incoming flow of M = 0.6 to a value of M=0.72 with an area ratio of A_{input}/A_{throat} = 1.10. Here the A (with subscripts) refers to the area of the sampler inlet (input) and to the area of the throat (the end of the taper) within the air sampler. The details of the thermodynamic effects of the accelerated flow on the compressible fluid (air with velocities greater than M = 0.3 should be treated as compressible) are not presented here. However, the subsequent cooling and pressure

reduction can be calculated from use of the equation below where A* is the sonic throat area where M = 1.

$$\left(\frac{A}{A^*}\right)^2 = \frac{1}{M^2}\left[\frac{2}{\gamma+1}\left(1+\frac{\gamma-1}{2}M^2\right)\right]^{(\gamma+1)/(\gamma-1)} \qquad (2)$$

Equation (2) is the appropriate classical equation for quasi-one-dimensional flow through a nozzle and is found in Anderson 's *Modern Compressible Flow* (3rd edition of 2003).

The amount of increased speed and cooling in the air sampler due to the taper is a function of Mach number of the flow and the pressure altitude of the mobile platform. Using Eq. (2) and the equation for the temperature and pressure for a standard atmosphere, one can calculate the impact on temperature. For a MTS with a TT sensor, the impact will be the increase in velocity [**increasing** temperature through Eq. (1)] and the **decrease** in temperature due to the cooling. These tend to offset each other and their combined effect is summarized in Table 3 below.

Delta T (degrees Kelvin) due to Air Sampler taper (function of height and Mach)

IH 40	0.00	0.01	0.02	0.04	0.06	0.11	0.20	0.33	0.57	1.06	3.28
IH 35	0.00	0.01	0.02	0.04	0.07	0.12	0.21	0.35	0.60	1.11	3.43
IH 30	0.00	0.01	0.02	0.04	0.07	0.13	0.21	0.36	0.63	1.16	3.59
IH 25	0.00	0.01	0.02	0.04	0.07	0.13	0.22	0.38	0.65	1.21	3.74
IH 20	0.00	0.01	0.02	0.04	0.08	0.14	0.23	0.39	0.68	1.26	3.90
IH 15	0.00	0.01	0.02	0.04	0.08	0.14	0.24	0.41	0.71	1.31	4.06
IH 10	0.00	0.01	0.02	0.05	0.08	0.15	0.25	0.43	0.73	1.36	4.21
IH 5	0.00	0.01	0.02	0.05	0.09	0.15	0.26	0.44	0.76	1.41	4.37
IH 0	0.00	0.01	0.02	0.05	0.09	0.16	0.27	0.46	0.79	1.46	4.52
Mach =	0.20	0.25	0.30	0.35	0.40	0.45	0.50	0.55	0.60	0.65	0.70

Table 3. Delta Temperature (K) for a TT sensor in air sampler with taper 1.1

The color scheme is as follows: the **blue** ordinate on the left is height in thousands of feet, the **red** abscissa on the bottom is Mach number (the flow is choked above M=0.7 and does not increase further), and the **black** numbers represent the likely values to be encountered by **commercial aircraft**.

The correction above is now only an approximation, just as the TT values were close, but approximate, as the effect of friction modifies the isentropic assumptions of equations 1 and 2. The same approximation applies to Table 4.

Delta Cooling (K) due to Air Sampler taper (function of height and Mach)

IH 40	0.34	0.55	0.84	1.20	1.67	2.27	3.06	4.14	5.71	8.30	17.0
IH 35	0.35	0.58	0.87	1.26	1.74	2.38	3.21	4.34	5.98	8.69	17.8
IH 30	0.37	0.61	0.91	1.31	1.82	2.48	3.35	4.53	6.25	9.08	18.6
IH 25	0.39	0.63	0.95	1.37	1.90	2.59	3.50	4.73	6.52	9.48	19.4
IH 20	0.40	0.66	0.99	1.43	1.98	2.70	3.64	4.93	6.79	9.87	20.2
IH 15	0.42	0.68	1.03	1.48	2.06	2.81	3.79	5.12	7.06	10.3	21.0
IH 10	0.43	0.71	1.07	1.54	2.14	2.91	3.93	5.32	7.33	10.7	21.8
IH 5	0.45	0.74	1.11	1.60	2.22	3.02	4.08	5.52	7.60	11.1	22.6
IH 0	0.47	0.76	1.15	1.65	2.30	3.13	4.22	5.71	7.87	11.4	23.5
Mach =	0.20	0.25	0.30	0.35	0.40	0.45	0.50	0.55	0.60	0.65	0.70

Table 4. Cooling (K) due to the taper in the air sampler of the MTS.

The MTS with two TS sensors (the final design) will not measure TT and thus the **cooling of the air at the nozzle entrance** will be a function of Mach number and pressure altitude as given in Table 4. This cooling factor is taken into account in the results as discussed in the next section.

3.5. The Ambient (TS) results from Run 04 and Run 03

The results for TSUW show the effect of the friction and other minor heat sources in the wind tunnel test area. The TSSS results are the ambient temperatures one is after with the MTS. These will contain the effects of the wind tunnel friction (not seen when flying in the real atmosphere), the effects of the friction due to the proximity of the air sampler to the aircraft skin, and the cooling effects of the taper in the air sample entrance.

The results from Figs.6 through 9 clearly show the rise of both TSUW and TSSS during the Mach number peaks. In each case the TSSS values are less than the TSUW values. The explanation is primarily due to the cooling effect of the air sampler taper which was discussed in Section 3.4 above.

The results in Table 5 below indicate the four cases where one can compare the maximum Mach number peaks (P) with the data from TSUW and TSSS from the MTS. Here, the results from Table 4 will come into play. The Table 4 values for the surface

(IH= 0) and for the interpolated values between the Mach number M=0.20and M = 0.25 will apply.

Event	Mach #	TSUV – TSSS	Cooling	TSSS (friction)
04 P1	**0.2357**	**0.30**	**0.67**	**0.37**
04 P2	**0.2415**	**0.45**	**0.71**	**0.26**
04 P3	**0.2350**	**0.32**	**0.67**	**0.35**
03 P1	**0.24881**	**0.33**	**0.75**	**0.42**

Table 5. Ambient Temperature (TS) and Effects of Friction

The first two columns are similar to Table 1 in Section 3.3. The third column is the difference between TSUW and TSSS at the respective peak in Mach number of column one. The fourth column is the interpolated value of cooling for that Mach number from Table 4. The last column is the additional air sampler friction effect (in temperature) calculated from the fourth column minus the third.

The additional friction seen is due to the proximity of the air sampler to the elongated model (surf board like metal extension) to which it is mounted. This friction will be stronger along the extended air particle trajectories across a real aircraft fuselage. The friction is not due to the flow inside the air sampler. This friction inside the measurement cell itself can be shown to be negligible for the short path inside the measurement cell by using the conventional equations for such viscous flow inside a duct.

The good news is that the combination of the cooling from the air sampler taper and the slower speed within the air sampler combine to keep the effect of friction low. However, whatever the effect of friction, it can be effectively modeled with the SVD approach coupled with sophisticated residual and outlier analysis. Thus, the correction itself from Table 4, which was used to help explain the resultant cooling, need not be explicitly calculated as the SVD approach will model this.

4. Modeling of TS and Accuracy Comparisons

This Section actually performs the ΔT friction modeling and compares the results of that modeling to the real data that was measured in the wind tunnel. Results from all runs are used and we begin with Run 04. Here the proper starting TS value is 13.921 and this is subtracted from the TS data: TSSS (i) = TSSS(i) – 13.921 which produces the SVD result of:

$$\Delta T = 0.35 \times 10^{-6} + 1.087\, M - 2.451\, M^2$$

which is consistent with the TSSS equation result of Section 3.1. Table 6 provides a summary of this Mach number correction applied to the data from Run 04 to produce the proper TS for all Mach numbers. There are 386 data points in this set and Table 6 takes us through the statistics of the differences from the [Mach corrected data – the actual data] in degrees C as residual analysis is applied at various levels.

Ztest	Mach data	# of data points	Average difference	STD of difference
1.00	**all**	**386**	**0.27×10^{-7}**	**0.0278**
0.96	**all**	**384**	**-0.11×10^{-6}**	**0.0272**
0.92	**all**	**382**	**-0.63×10^{-6}**	**0.0266**
0.88	**all**	**381**	**-0.15×10^{-7}**	**0.0263**
0.84	**all**	**379**	**0.40×10^{-7}**	**0.0256**
0.84	**M > 0.20**	**110**	**0.79×10^{-3}**	**0.0296**
0.84	**M > 0.21**	**90**	**0.20×10^{-2}**	**0.0281**

Table 6. Mach correction: TS data from Run 04 compared to actual data from 04.

The last two columns of Table 6 indicate the average difference of all the data points and the standard deviation of the difference (STD). One can see from the results of Table 6 that the results are **extremely accurate** and remain so when only the largest Mach numbers are used in the statistics (as seen in the last two rows of Table 6). The results are well below our goal of a STD of < 0.3 [or better than twice the accuracy (0.6 to 0.8 degree C) of the Goodrich probe in the best of conditions].

The next step is to compare this Mach correction for the Run 04 and use it with the long Run 03 data. We do that below, but earlier we cautioned that the Run 03 data set was poor from a mathematical perspective as Fig. 8 indicated that the wind tunnel controls slowly allowed the Mach number to drift downward slightly at each of the desired "stationary" levels before increasing in value to the next level. This produced a very poor data set from a mathematical and physical perspective. **Mach numbers decreasing with temperatures increasing-- produces many inconsistent data points.**

A larger issue is the degree of difference in the polynomial fits of the data. This is a severe test of the methodology as one would never use such a data set to do what we are trying to do. Nevertheless, we show that even in this severe test one can achieve a satisfactory result with the methodology employed.

Table 7 indicates the same information as Table 6 but now using the Run 04 polynomial correction for the Run 03 data. There are 2019 data points in this long run. One observes

that the low Mach numbers (at the beginning of the ramp up **in the data used** and at the end of the ramp up) have errors as large as 0.7 degrees C. Thus, only when the residual analysis removes 54% of the maximum error data does one obtain the desired goal of a STD of < 0.3 degrees C.

Ztest	Mach data	# of data points	Average difference	STD of difference
1.00	**all**	**2019**	**0.004**	**0.6049**
0.94	**all**	**1849**	**0.082**	**0.5652**
0.84	**all**	**1475**	**0.047**	**0.4906**
0.74	**all**	**1183**	**0.018**	**0.4139**
0.64	**all**	**973**	**0.017**	**0.3475**
0.54	**all**	**803**	**0.016**	**0.2893**

Table 7. Results for Run 04 Mach correction compared to actual data from Run 03.

The next two sets of calculations are for the TT data from Run 04 and Run 07. Recall that this TT data is approximate from the true TT as the conditions for isentropic flow are not realized as discussed before. The results from Run 04 using the Mach correction from the TT data (TTSS) to find the static temperature (TS) are shown in Table 8. The results are very accurate, not quite as good as the results from the TS data shown in Table 6, but certainly well below the goal of a STD of < 0.3 degrees C.

Ztest	Mach data	# of data points	Average difference	STD of difference
1.00	**all**	**386**	**-0.18×10^{-6}**	**0.0768**
0.96	**all**	**381**	**-0.22×10^{-6}**	**0.0748**
0.92	**all**	**379**	**-0.73×10^{-7}**	**0.0740**
0.88	**all**	**375**	**-0.142×10^{-7}**	**0.0726**
0.84	**all**	**370**	**0.32×10^{-6}**	**0.0708**
0.84	**M > 0.20**	**110**	**0.13×10^{-2}**	**0.0734**
0.84	**M > 0.21**	**88**	**0.86×10^{-2}**	**0.0731**

Table 8. Mach correction: TT data from Run 04 compared to actual data for 04.

The final comparison is to the polynomial data from the TT data of Run 07 with the TT data from Run 04. In this case we have a TS value of 13.90 from Run 04 and an M = 0 value from the polynomial of TT of Run 07 of 14.26 (see SVD values in Section 3).

In order to obtain the [Mach corrected data – the actual data] for this case, one must make two adjustments. The first is the TTSS = TTSS -14.26 + 13.90 = TTSS – 0.36. However, there is no TSSS data from Run 07 (only TSUW data) so a second adjustment is required since the TSUW data from Run 07 is 0.22 warmer than the TSUW data from Run 04 (see SVD values of Section 3). Thus, the total adjustment in Run 04 TT data is TTSS = TTSS – 0.36 + 0.22. The results are shown in Table 9.

Ztest	Mach data	# of data points	Average difference	STD of difference
1.00	**all**	**386**	**0.013**	**0.2077**
0.98	**all**	**384**	**0.010**	**0.2058**
0.94	**all**	**383**	**0.009**	**0.2048**
0.90	**all**	**378**	**0.004**	**0.2005**
0.86	**all**	**370**	**-0.005**	**0.1936**
0.82	**all**	**362**	**-0.014**	**0.1864**
0.78	**all**	**356**	**-0.020**	**0.1812**
0.74	**all**	**350**	**-0.027**	**0.1760**

Table 9. Mach correction: TT data from Run 07 compared to actual data for 04.

The results from Table 9 indicate that the **transfer of Mach correction produced from one data set is transferable to another data set.** This is, of course, what must happen in the real world. The last row of Table 9 indicates that our STD is nearly twice as good as our goal when only about 10 % (36 of 386) of the data points have been removed by the residual analysis.

The next phase of testing requires the MTS on a research aircraft (two options are currently being pursued. The aircraft must have an accurate TS or TT sensor that can be recorded along with the two TS sensors from an MTS. This aircraft test, performed in parallel with other uses of the aircraft, will provide a **much larger** data set from which to obtain the effects of friction as a function of Mach number in some polynomial form.

5. Summary and Conclusions

The UWAL wind tunnel tests verified several important aspects of the current MTS design. These results are summarized here and a final recommendation is made on the next steps before flying the MTS on an aircraft.

The temperature sensors, the two in the MTS and one in the hybrid system, were very sensitive to change with a quick response time. The absolute values of the temperatures (their amplitudes through all phases of the various runs) stayed within their bounds (i.e., TSSS < TSUW < TTSS for all Mach numbers) throughout all the runs.

The total temperatures from Runs 03 , 04, and 07 were very close to the values expected as seen in Table 1. Here the initial value of temperature (TS) in Eq. 1 had to be determined from the SVD model fit to the data because of the initial cooling within the measurement test area of the tunnel.

The ambient temperature measurements from the MTS (TSSS) from the various runs were quite consistent. The additional friction effect (shown in Table 5) was reasonably consistent considering the relative inaccuracy of the TSUW data which contributes to the calculated additional friction.

The TSSS values are the final product of the MTS measurement system. Currently, the situation in the aviation world is that the measured TT values on aircraft are used to determine the TS values appropriate to the atmosphere. These TS values are not as accurate as required, are subject to large random errors and biases, and have occasional biological induced biases. The protected TS sensor in the MTS is a significant design advantage for sensor accuracy and sensor lifetime.

Since all aircraft have pitot tubes that measure static (PS) and total (dynamic) pressure (PT), the Mach number can be calculated from the relation:

$$PT = PS (1 + 0.2 M^2)^{3.5} \qquad (3)$$

Thus, the aviation need for TT can be met from the direct and accurate calculation of TS via the MTS, the measured Mach number from Eq. 3, and the use of Eq. 1. **The atmospheric science use of TS can be made directly without all the problems of the Goodrich TAT probe.**

The accuracy of the TS measurement depends the modeling of the friction effect. The initial temperature sensor measurement within the MTS itself begins about 6 times as accurate, 0.1 compared to 0.6 C (in the best of conditions for the TAT probe), as the final heated TAT probe derived TS measurement. The isolation of the friction effect by the MTS design and the subsequent modeling of the friction effect as a polynomial in Mach number via the SVD method assures a final accuracy of 2 to 3 times that of the Goodrich TAT probe (in the best of conditions for the heated TAT probe).

The above claim is based upon many simulations performed with a large variety of error conditions introduced. The final modeling is enhanced by residual and outlier analysis. Such analysis was performed here for the different modeling of the temperature values TSUW,TSSS, and TTSS. The residual analysis used was quite simple. The results of Section 4 indicate that both TS and TT sensors could be used within the MTS to achieve our goals. The TS results were slightly better and more appealing to use than the TT results in view of the theoretical lack of rigor of the TT results in a viscous environment.

In the actual modeling of the friction effect with real aircraft data (with independently measured TS and MTS values provided), **the proprietary residual analysis** is far more sophisticated than was described and implemented here is this summary of the test results. **Nevertheless, the results of Section 4 indicate that even the simple residual analysis improved the results shown there. These results were good enough to indicate that the friction modeling was successful and within the simulation range of results seen before. This assures us that the MTS can meet the accuracy demands we have set.**

There was an offset required between TSSS and TTSS that was consistent throughout the runs. This was due to a final known change in the circuit board design which serves both temperature sensors. The offset was only **0.15** degrees C. **This is a small value but the goal of this sensor is extreme accuracy!** The offset will be removed with the next MTS upgrade. The upgrade involves using slightly more expensive low temperature coefficient resistors (temperature coefficient of 2 ppm / C versus the 100 ppm / C currently used) and an improved design that isothermally mounts the "surface mount" resistors as a group on the circuit board.

The inertial separator for the MTS need not be as effective as for the WVSS-II. Thus the taper will be made less with the area ratio reduced: $A_{input} / A_{throat} = 1.05$. This will make the temperature correction values of Table 4 substantially reduced. A final recommendation is to design the next MTS with two sensors inside the walls of the air sampler measurement area with no TT sensor in the interior of the area. This allows the backup sensor that the Goodrich system has and affords the best accuracy.

An extremely important further advantage of the two TS sensors is their protected position within the walls of the measurement area. This allows a much longer sensor lifetime for the MTS to perform the measurement task of the ambient temperature.